

# Base metal and Uranium mineralization in the Gröden/Val Gardena Sandstone of South Tyrol

→ Helmut Wopfner<sup>1</sup> & Joe Drake-Brockman<sup>2</sup>

<sup>1</sup> Geology Department, University of Cologne, Germany; e-mail address: h.i.wopfner@t-online.de

<sup>2</sup> DB-GEOINFO P/L, Perth, West Australia; e-mail address: dbg@dbgeoinfo.net.au

## ABSTRACT

The Gröden/Val Gardena Sandstone of the central and eastern Southern Alps succeeds the early Permian rift volcanics (Bozen/Bolzano and Lagorai Volcanics or Athesian Volcanic Group). In the surrounds of Bozen/Bolzano the Gröden/Val Gardena Sandstone is largely a red bed succession, comprising in ascending order, wedges of grus debris and other weathering materials, followed by gypsiferous red beds of inland sabkhas, then a succession of stacked, fining upward sequences of meandering stream origin with all facies associations of such an environment. The formation is topped by interbedded sandstones and red beds of estuarine, delta and coastal plain origin. The Gröden/Val Gardena Sandstone of this region frequently contains base metal and uranium mineralization, which extends from Grissian/Grissiano via Tschöggelberg and Regglberg to the Bletterbach. Two types are known: in the lower part of the section, iron, copper and uranium, brought in by alkaline oxidized ground waters came in contact with reduced zones sustained by decomposing plant matter. Framboidal pyrite (iron), covellite (copper sulfide) and tennantite (copper arsenate) filled undeformed cell lumina in rotting plants, while uraninite was fixed intergranular or as diffuse blebs, causing reaction halos in coal. Higher up in the section pyrite, galena (lead), sphalerite (zinc) and minor tennantite impregnated the pore space of carbonaceous sand and siltstones in acid, reducing environments formed in the mixing zone between marine and terrestrial ground waters. Tirolite (Ca-Cu hydrated arsenate) and the copper carbonates malachite and azurite were formed as visible weathering minerals.

## KEY WORDS

ore concentration, iron, lead, copper

## 1. INTRODUCTION

The steep and often vertical flanks of the Etsch/Adige Valley between Meran/Merano and Auer/Ora and of the Eisack/Isarco Valley between Waidbruck/Ponte Gardena and Bozen/Bolzano are formed by the early Permian, dominantly acidic, volcanic suite of the Bozen/Bolzano Volcanics (originally 'Bozner Quarzporphyr' = Bozen/Bolzano quartz porphyry, but recently termed the Athesian Volcanic Group). Roughly 850 m to 1100 m above the valley floor there is a marked bevel, leading to a more subdued and flatter morphology. This change is caused by the middle to late Permian red bed succession of the Gröden/Val Gardena Sandstone or Gröden/Val Gardena Formation which overlays the rocks of the Bozen/Bolzano volcanic suite (Fig. 1). The lower Gröden/Val Gardena Sandstone in this region often exhibits small outcrops of bright green and blue coloured encrustations of the secondary copper minerals tirolite, malachite and azurite as shown in Figure 2. These are typical gossan minerals indicating the presence of copper sulphides beneath the surface. They are also commonly radioactive indicating the presence of uranium. In addition, numerous occurrences of lead and zinc are known. Some of this mineralization has been exploited in the past. Various occurrences were discussed, amongst others, by Mittempergher (1974), Brondi et al. (1973), Haditsch & Mostler (1974), Fels (1979), Griesbeck (1979), Koch (1979), Wopfner et al. (1983), Drake-Brockman (1988), Drake-Brockman & Wopfner (1988). Important ore concentrations in the wider surrounds of Bozen/Bolzano occur in the Prissian/Prissiano Forrest north of Payers-

bach, in several sections of the Tschöggelberg, especially near Mölten/Meltina and Jenesien/San Genesio, around Deutschnofen/Nuova Ponente on the Regglberg, and in the UNESCO World Heritage site, the famous gorge of the Bletterbach (Drake-Brockman, 1988) (Fig. 1). Very much simplified two types of ore deposits may be distinguished: A copper/uranium association and a lead/ zinc mineralization. Pyrite is present in both types of mineral systems, but it also occurs independently, usually in association with plant matter incorporated within the sedimentary deposits.

## 2. REGIONAL SETTING

The Permian rock sequences of the Southern Alps reflect the transformation from the Variscan consolidated continental crust to the depositional realm of the nascent Tethys. Generally assumed to have progressed from east to west, this process was initiated by thermal bulging and overstretching of the crust, causing the formation of complex rift structures as suggested by Wopfner (1984) and subsequently expanded on and modified by Cassinis (1986), Venturini (1990), Massari et al. (1994) and others.

Initiation of the rift systems in the Cisuralian (early Permian) was accompanied by widespread volcanism. Commencing with basic to intermediate igneous effusions, it culminated with the expulsion of rhyodacitic ignimbrites, lavas and ash falls which, in the Etsch/Adige Basin, lead to the accumulation of up to 3,000 m of volcanic and volcano-sedimentary rocks. Elsewhere, as in the

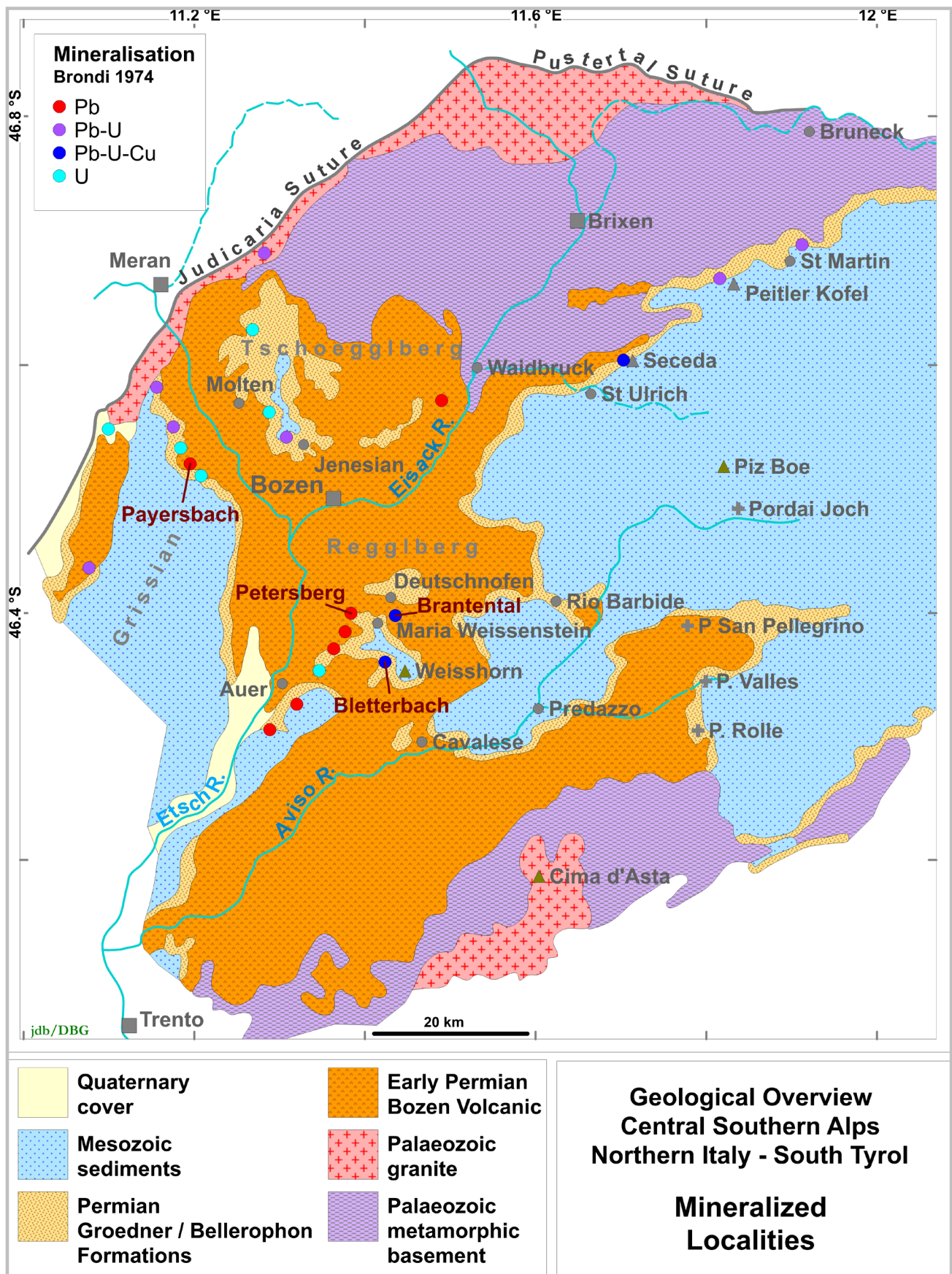


FIG. 1: Generalized geological map of the area under discussion, showing sites of ore mineralisation and localities mentioned in text.





**FIG. 2:** Secondary copper minerals (tirolite and malachite) on the surface of Gröden/Val Gardena Sandstone indicate the presence of copper mineralisation. Specimens were taken from an exposure east of the homestead Steinmetz, south of the monastery Maria Weissenstein, situated about halfway between Weisshorn/Corno Bianco and Brantental.

basins west of the Judicaria Line, lavas and ignimbrites were less prevalent, the volcanic facies being dominated by volcanoclastic deposits (Cassinis et al., 1975, 1994).

East of the Dolomites direct evidence for volcanism is lacking, but cobbles and pebbles of rhyolitic ignimbrites incorporated in the Gröden/Val Gardena Sandstone as far east as Slovenia, suggest that active volcanism had existed within the source areas of the Gröden/Val Gardena Sandstone of these regions (Drovenik, 1983; Kober, 1983, 1984; Venturini, 1990).

After a hiatus of uncertain duration (see below), the volcanic complex of the early Permian was succeeded by the Gröden/Val Gardena Sandstone. This rock sequence represents the depositional event leading from the almost entirely terrestrial environment of the early and middle Permian to the marine conditions of the late Permian Bellerophon Formation. The Gröden/Val Gardena Sandstone resulted from a great variety of depositional environments which are described below.

The Bellerophon Formation, rich in dolomites, gypsum and algal mats, was laid down in a hot evaporative climate (Bosellini & Hardie, 1973). It terminated the Permian depositional event in the central Southern Alps. Sedimentation continued uninterrupted into the Triassic, providing classical sites of the Permian/Triassic boundary like that at Tesero in Val Fiemme (Società Geologica Italiana, 1986). The Permian succession of the Dolomites can be traced in subsurface far south beneath the Venetian Plain where rocks of the Bellerophon Formation, Gröden/Val Gardena Sandstone and of the volcanics were intersected in the petroleum exploration well Legnaro 1 between 4,510 m and total depth at 4,989 m.

### 3. HOST ROCKS OF ORE DEPOSITS

#### 3.1. Depositional environments

The formation of the ore concentrations within the Gröden/Val Gardena Sandstone was linked to specific sedimentary environments described, amongst others by Buggisch (1978), Griesbeck (1979) and Massari et al. (1994). Within the surrounds of Bozen/Bolzano the overall successions of the formation are fairly similar and generally comprise four distinctive facies associations or sequences. However, the presence or not of the lower members is strongly influenced by the topography of the palaeo-surface on which the Gröden/Val Gardena Sandstone was laid down, a fact not generally recognized by other wor-

kers. Elevation differences between high and lowland, inherited from the volcanic era or due to syngenetic faulting, usually are in the order of several decametres and may exceed 150 m. This also influences the total thickness of the Gröden/Val Gardena Sandstone. In the Bletterbach for instance, it measures 230 m whereas around Maria Weissenstein, less than 2 km to the north its thickness averages less than 80 m which then increases in the upper Brantental (Kehr Graben), situated 4 km further north to 140 m.

As mentioned above, four facies systems or third order sequences may be distinguished. Our sequence identification differs from those of Italian workers as for instance Massari et al. (1994) which do not recognize the basal grus and weathering sequence as a separate subdivision.

**Sequence 1:** The basal unit consists of *in situ* disintegrated weathered material of the underlying ignimbrites, generally referred to as grus. This is a typical weathering product of hot and arid environments. It is characterized by generally subangular, grit sized grains of volcanics derived by physical disintegration, cemented by ample matrix of maroon colour. The colour is due to hematite and other iron oxides forming an opaque cement. Microprobe analyses demonstrate an appreciable participation of leucoxene in the opaque matrix. These are important aspects, because copper released by the break down of silicates can not be integrated into the lattice of hematite and the mobilisation of titanium points to strong oxidizing conditions (Force, 1976). The grus deposits (Fig. 3) either form sheets or wedge shaped bodies increasing in thickness from palaeo-highs towards morphological lows. Their geometry resembles that of fan deposits, increasing in thickness centrifugally from the palaeo-highs.

Palaeosoils are quite abundant in many areas, whereby vertically textured calcretes are particularly frequent near the base of the grus sheets. The formation of calcretes requires alkaline conditions with pH values between about 9 and 11 and sufficient fluids for the mobilisation of the carbonates. Such conditions indicate a hot climate, but one in which aridity was moderated by ephemeral precipitation (Wopfner & Farrokh, 1986). Typical examples of this lithofacies are exposed on the road from Deutschnofen/Nuova Ponente to Petersberg/Monte San Pietro as depicted in Figure 3 and around the northern limit of Petersberg/Monte San Pietro village.



**FIG. 3:** Red grus (sequence 1), forming the base of Gröden/Val Gardena Sandstone, rests unconformably on Early Permian rhyolitic ignimbrite at the road from Petersberg to Deutschnofen at the upper Brantental (see Fig.1). Calcrete palaeosoils, recognisable by their vertical texture are in the left of picture, about 30 cm above the unconformity. Scale on hammer in inches.



**Sequence 2:** The next lithofacies system is dominated by dark purple, commonly gypsiferous siltstones with thin intercalations of layers of fine grained, often festoon bedded sandstone. This facies unit either overlays the grus sheets or, especially on morphological highs, rests directly on smooth surfaces of ignimbrites, as for instance in the Bletterbach, about 300 m downstream from the waterfall (Fig. 4). Occasionally a layer of lag gravels may be present at the base of this unit.

The cloudy to botryoidal shaped bodies of gypsum aggregates contained within the red siltstone vary between 5 and 20 cm in diameter (Fig. 4). Their form and mode of occurrence indicates that their emplacement was caused by evaporative pumping, a typical process of hot and arid environments. It identifies this unit as typical sabkha deposits. Higher up braided stream deposits may be intercalated and stratified gypsum occurs interbedded with siltstones or fine grained sandstones. Near the contact with the grey sandstones of sequence 3 such layered sandstone-gypsum packets were locally deformed by progressive loading caused by rapid deposition of fluvial sands of the overlying facies system.

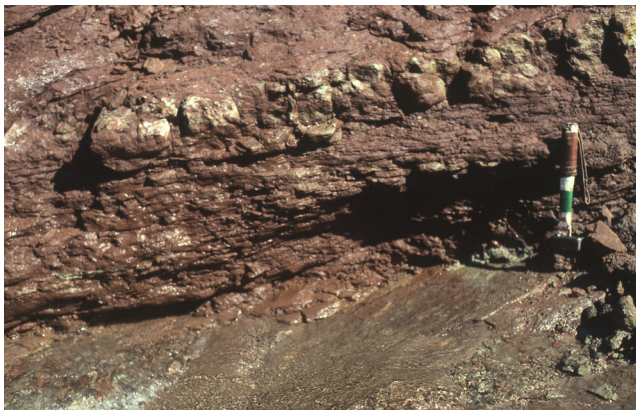


**FIG. 4:** Red, gypsiferous siltstone of sabkha origin of sequence 2 deposited directly on a smooth surface of ignimbrite of the Bozen Volcanics in the Bletterbach. Scale on hammer in centimetres.

**Sequence 3:** This is the most prominent facies system and may exceed 80 m in thickness. It is a stacked sequence of grey, medium to coarse grained sandstones and purple siltstones, forming sheer walls in the canyon of the Bletterbach (Fig. 5). The sandstones are point bars of meandering streams or sheet flood deposits, whereas the siltstones derived in overbank clay pans and playas. The sandstones show both, parallel and current bedding and occasionally exhibit load casts at their base. The streams were ephemeral in nature, but retained a permanent intergranular flow below the surface. Such an environment is indicated by green reduction halos emanating from the base of the grey sandstones down into the underlying, purple siltstone of the clay pan deposits as much as 1 m. Decaying plant matter within the sandstones created pronounced negative Eh pore fluids which invaded the red siltstones below, thereby reducing hematite and other iron oxides of the red siltstones. The latter are characterized by high  $\text{Fe}_2\text{O}_3$  and low FeO values, the ratio being about 4:1. Within the green halos however, not only  $\text{Fe}_2\text{O}_3$  is reduced drastically, but the total iron content is much reduced, suggesting that during the process of early diagenetic colour change iron was removed from the system (Press, 1982). This is but one example of the many microenvironments cre-



**FIG. 5:** Exposure of sequences 3 and 4 in the inner canyon of the Bletterbach forming sheer walls, about 200 m downstream from the Butterloch waterfall. Cut and fill structures are recognisable at the base of the bold sandstone with the brown surface colour. This sand is topped by red playa deposits, exhibiting a reduction halo at the top. The base of sequence 4 is roughly at the lowest trees on the left side of the picture.

ated by changes of pH and Eh, influenced by the varying input of plant material, intensity of aridity and evaporative pumping and soil formation. Low pH cells, created by the decay of ample plant material for instance led to the transformation of feldspars to kaolinite and the release of silica, whereas high alkaline conditions in response to long aridity fostered carbonate cement and the formation of carbonate concretions (Griesbeck, 1979; Drake Brockman, 1988).

The third facies cycle is concluded by the so called 'Cephalopod Bank', a grey, medium grained, calcareous sandstone, varying between 1.5 m and 2 m. It is of deltaic origin as evidenced by nautiloid fossils, first described by Mutschlechner (1933). Immediately below this sandstone is a very characteristic sequence of coal, carbonaceous mudstone and calcareous concretions, recognisable also in areas where the calcareous sandstone is absent or very thin.

**Sequence 4:** The succession above the 'Cephalopod Bank' measures about 45 m to 50 m and consists of a succession frequently alternating between red mudstones and siltstones and grey to fawn sandstones (Fig. 5). The redbeds represent deltaic, infra to supratidal, lagoonal and mudflat deposits whereas the current bedded sands, frequently cut into the underlying sediments, originated from distributary channels or crevasse splays. The sandstones contain accumulations of plant debris,



providing foci of ore concentrations. The proximity of the sea is evident by occasional foraminifera (Buggisch, 1978; Griesecke, 1979) and by the presence of sand pseudomorphs after Hopper crystals of halite. Local abundance of varied tetrapod footprints indicates a congenial environment for reptiles in a hot, semiarid to arid climate on near-shore mudflats (Conti et al., 1977). Intercalated, yellow coloured yoghurt dolomites, typical for barrier lagoons, herald the transition to the tardo-Permian evaporate deposits of the Bellerophon Formation.

### 3. 2. Coal and thermal maturity

Coal is present in all facies associations except for the basal grus deposits. It forms mostly as lenses composed dominantly of vitrinite of 5 cm to 20 cm thickness but also as discrete masses of coal derived from individually coalified trunks or branches. The latter type is frequently associated with framboidal pyrite and diagenetic gypsum, not to be mistaken with that of evaporative origin. Further types of coal occurrences originated from accumulations of plant debris in current bedded sands of meander or distributary channels which are common within the uppermost part of the sequence. Finely disseminated plant material occurs in black, more or less bituminous mudstones of overbank swamps. The type of occurrence indicates that practically all of the coals are allochthonous, derived from driftwood and other plant material which originated primarily from gallery forests edging the channels. Wartmann & Knatz (1977) who investigated coals from the Bletterbach and from the base of the Seceda found that the coals consist almost entirely of vitrinite, composed of about equal parts of telinite and colinite. The complete lack of the maceral cutinite in individual coal seamlets (but not in plant detritus), further supports a driftwood origin. Of special interest is the identification of charcoal derived from wildfires at the time of deposition (Uhl et al., 2012).

The rank of the coals as indicated by percentage of vitrinite reflectance, indicates the maximum temperature to which the organic material and the surrounding strata were exposed. Coals within the Gröden/Val Gardena Sandstone in the Bletterbach have an average vitrinite reflectance of  $R_o$  0.53%. On the Tschöggelberg vitrinite reflectance averages  $R_o$  0.56% at Jenesien/San Genesio and  $R_o$  0.63% at Mölten/Meltina (Bielefeld, 1998). Schulz & Fuchs (1977) report reflectance values for coal samples from Prissian/Prissiano near Payersbach between  $R_r$  0.44% and 0.64%. Such values correspond to the beginning of the oil generation window and are indicative of a temperature exposure of about 60° C to 75° C. Vitrinite reflectance increases slightly towards the east, accounted for by the influence of the middle Triassic intrusions and volcanoes centred around Predazzo.

Several coal samples from the Bletterbach, but also from the Brantental and from the northern base of the Seceda show strongly reflecting reaction haloes surrounding minute crystals which could not be identified microscopically (Fig. 6). X-ray fluorescent analyses identified uranium and iron to be the only metals contained in that coal (Wartmann & Knatz, 1977), wherefore the crystals in the centres of the haloes must be a uranium mineral, possibly coffinite (uranium silicate). Coals with such reaction haloes show elevated vitrinite reflectance values up to  $R_{max}$  0.88% (Griesecke, 1979). This may have been the reason for excessively high reflectance measurements of up to  $R$  1.8% reported by Buggisch (1978). A special feature of the Gröden/Val Gardena Sandstone, especially on the Tschöggelberg is the diagenetic formation of Dawsonite and Nordstrandite (Wopfner & Höcker, 1987).

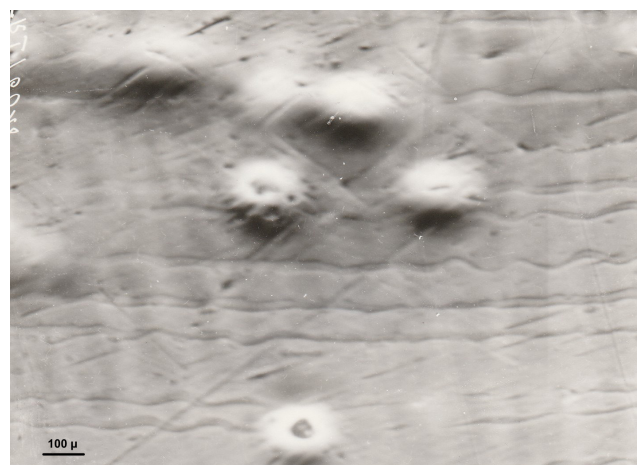


**FIG 6:** Microphotograph of reaction haloes with marked elevated reflectivity surrounding radioactive crystals in a coal from Seceda, near St. Ulrich, Groeden Valley. (Oilimmersion, magn. 220x, photo by Wartmann & Knatz, 1977).

### 3.3. Age of the Gröden/Val Gardena Sandstone

The hiatus between the top of the Bozen volcanics and the base of the Gröden/Val Gardena Sandstone is generally assumed to encompass about 10 million years (e.g., Brantner & Keim, 2011). This interval was also a time of tectonic readjustment as indicated by the incorporation of cobbles of early Permian Trogkofel Limestone within the basal Gröden/Val Gardena Sandstone of the north-eastern Dolomites and the reworking of the volcanics. Using the numerals cited by Brandner & Keim (2011), deposition of the Gröden/Val Gardena Sandstone would have commenced around the Wordian/Capitanian boundary. Massari et al. (1994) place the onset of deposition at the early Tatarian, considered at that stage to be in the later part of the Capitanian. At the present, palaeo-biological evidence suggests a Lopingian age for the major part of the formation (Nicosia et al., 2001; Kustatscher et al., 2012). Cassinis & Ronchi (2001) also argued for a late Permian age. The solution of the apparent contradiction may be found in the diachronic beginning of sedimentation and the lack of biological evidence in the grus of the very basal deposits of the formation. Within the area of discussion, the time span of apparent non-deposition between the termination of volcanism and the onset of deposition was a period of weathering, soil formation and slow terrestrial sedimentation in a hot and arid environment that occasionally received sufficient precipitation for the mobilisation of carbonate and titanium.

On palaeo-highs where the original surface of the volcanic rocks has been preserved, there is clear evidence for long-lasting weathering processes in a hot and arid climate. Such evidence comprises open sheeting-joints, core-stones and round, grus-filled solution pits with overhanging lips known by the Australian Aboriginal term “gnamma” (Wopfner & Farrokh, 1986). This situation contrasts with that in palaeo-depressions, where several decametres of grus form aprons around the highs. In many instances it is quite difficult to draw a boundary line between volcanic rocks, weathered volcanics and the overlying grus sheet, a phenomenon already observed by Andreatta (1959). Adding the long time elapsed during the formation of the grus-blankets, the deposition of the Gröden/Val Gardena Sandstone may well have commenced in the Guadalupian.

The magneto-stratigraphic event of the Illawarra Reversal was identified in the Paularo section (Mauritsch & Becke, 1983) and

also in the section at the foot of Seceda (Dachroth, 1988). According to Menning (2001a, 2001b) this magnetic event occurred at 265 Ma, placing it at the boundary between Wordian and Capitanian. Nicosia et al. (2001) have cast doubt onto the validity of the palaeomagnetic data, but in view of the diachronous nature of the onset of deposition, the much greater thickness of the formation in the Carnia region (Paularo and Forni a Voltri, see Ventorini, 1990) and the long duration of grus deposition, such criticism appears too severe. As Assereto et al. (1994) suggested, we can only judge after additional palaeomagnetic investigations.

3.4. Ore deposits

The distribution and types of ore deposits within the Bozen area is shown on Figure 1. In the gorge of the Bletterbach the stratigraphically lowest ore mineralization occurs in red, oxidized sandstone of sequence 2, only a few meters above the top of the Bozen Volcanics. The deposit was mined, apparently in the 18<sup>th</sup> century, hence the name of the locality: ‘Knappenlöcher’, meaning ‘miners holes’.

On the surface the mineralized zone is indicated by patches of limonite derived from weathered pyrite and incrustations of azurite and malachite. However, the most striking feature is a reduction front within which the originally oxidized, red sandstone has been completely bleached. Measurements of radioactivity on the outcrop with a lead shielded scintillometer (SPP2) gave readings between 150 to 100 cps (counts per second) (Fig. 7). The old miner’s adit which was still accessible in

the mid 1980’s revealed the target of the old miners: A large coalified tree trunk of 3 to 4m length, exposed in the sandstone of the roof of the drive. The sandstone in the immediate vicinity of the coalified trunk shows patches of green and blue stains caused by secondary copper minerals. The coal of the trunk itself is impregnated with covellite (copper sulfide) and tennantite. What the miners did not know was the presence of uraninite and other uranium minerals. Covellite and tennantite fill the practically undeformed cell lumina of the wood. Uranium is present as uraninite, either associated with pyrite, or diffusely distributed in coal, recognisable only by the reaction halos within the surrounding coal.

Griesecke (1979) who, to the best of our knowledge, presented the first comprehensive stratigraphic and petrographic inventory of the Bletterbach succession, surveyed the old mining drives in 1976 and measured the radioactivity within the adits with an unshielded scintillometer. She obtaining values in excess of 2,000 cps (Fig. 8). The hot spot was within the mineral impregnated, fossil tree trunk in the roof of the adit, for which she calculated the U content of the coal at 800 ppm.

An excellent example of Cu/U mineralization is exposed in the neighbouring Brantental, about 2.5 km south of Deutschnofen/Nuova Ponente. The exposures are situated in the ravine forming the uppermost part of the valley, locally referred to as ‘Kehr Graben’. They present convincing evidence for the dependence of the mineralization on plant matter as demonstrated in Figures 9A and 9B. Figure 9A shows a small coal seam in bleached sandstone, surrounded by ellipses of iso-radiation lines of

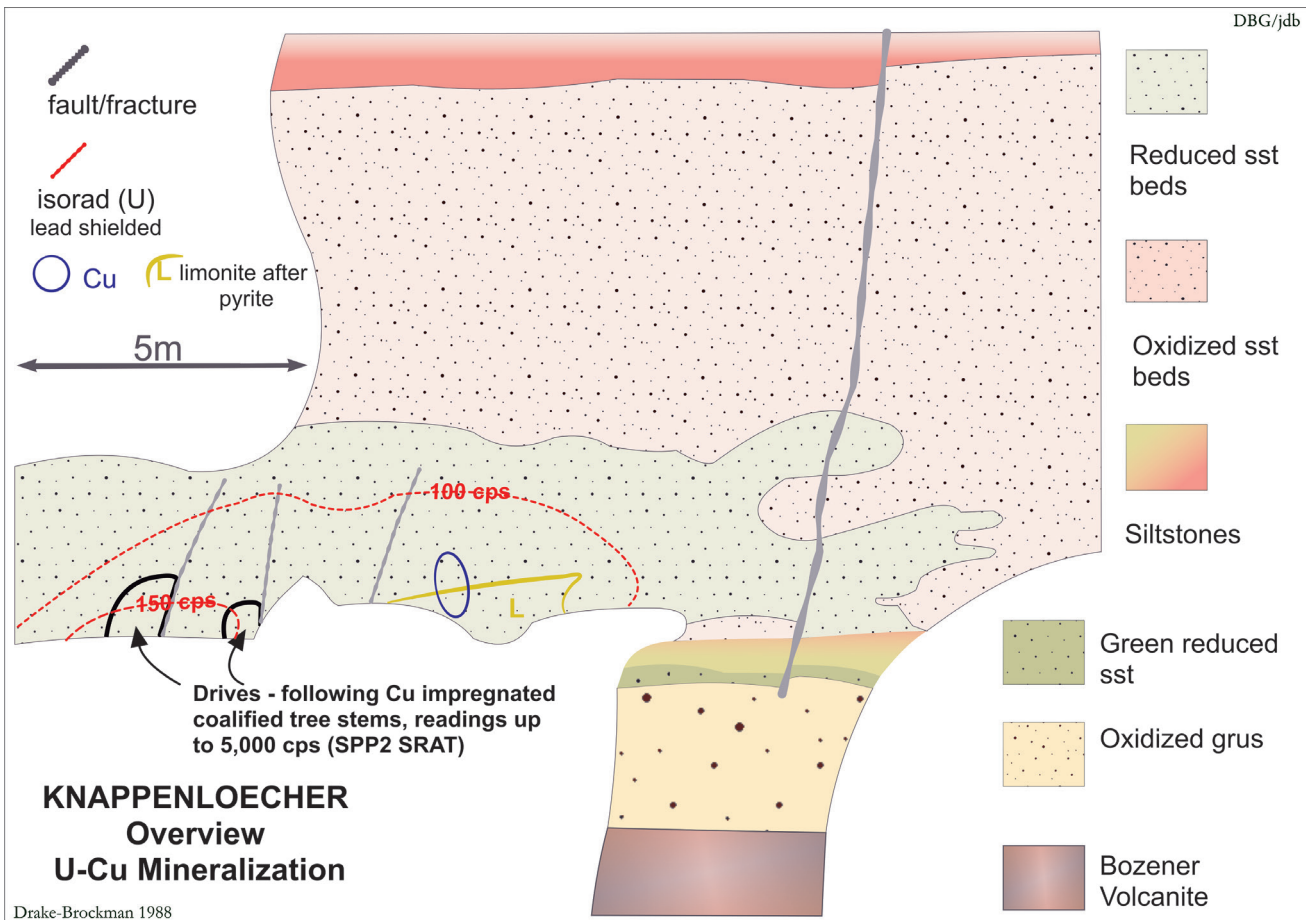


FIG. 7: Colour changes of the exposures around the Knappenloch and radioactivity in counts per second (cps) at the outcrop (modified from Drake-Brockman, 1988).



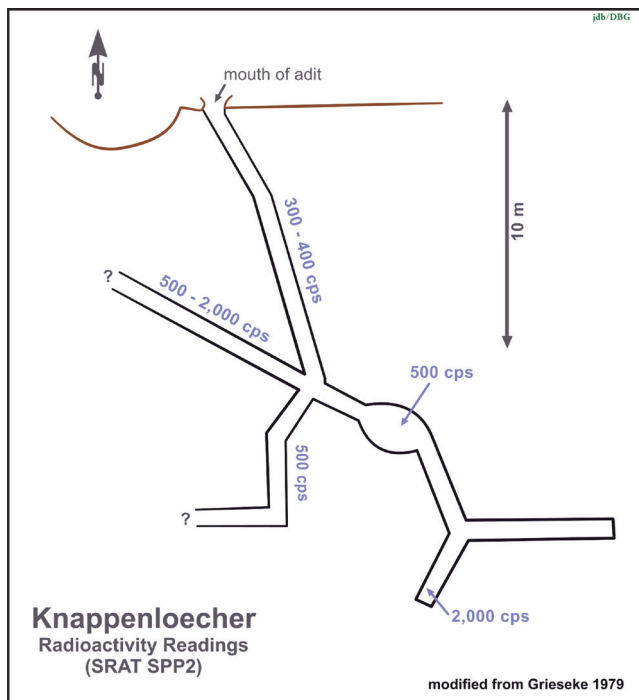


FIG. 8: Plan of the adits of Knappenloch and intensity of gamma-radiation shown in counts per second (cps), measured in the various sectors of the adits (modified from Grieseke, 1979).

diminishing intensity. Similarly, copper mineralization forms a halo around the coal seam. Figure 9B shows a coal seam a few meters distant from the first with similar features as the first example, but here the reduction front within the originally red, oxidised sandstone is clearly recognizable. The block diagram of Figure 10 summarises the situation. It shows both sides of the ravine and the positions of the outcrops 9A and 9B and the magnitude of the reducing system within the reddish, oxidized sandstones which was responsible for the creation of the U/Cu mineralisation. The main ore minerals are again covellite, tennantite, uraninite and pyrite.

The primary copper mineralisation is tennantite intergrown with covellite. The mineralisation occurs as 0.1–0.2 mm sized impregnations in the sandstone matrix, as pseudomorphs of wood cell lumina (0.05 mm) and as pseudomorphs of liptinite knots in coal (0.3 mm). Microprobe analyses of tennantite gave the following compositional range: Cu: 41–57%; As: 10–20%; S 10–24%, Zn: 6–10%; Fe: 1–2%; Sb: 0–5%. Covellite analysed at Cu: 67% and S: 33% which corresponds closely to the norm. Trace amounts of chalcopyrite and chalcocite were also noted.

The mineralisation took place after initial pyrite precipitation, but before compaction and coalification of the organic material (Fig. 11). Examples of strong U and Pb mineralization associated with a clear redox front exists in the Prissian Forrest, near Payersbach. The exposures at Mölten/Meltina and Jenesien/San Genesio also harbour similar types of mineralisation that include galena with lesser amounts of sphalerite, uraninite, very fine U-Ti mixtures (probably inter-grown uraninite and uranium

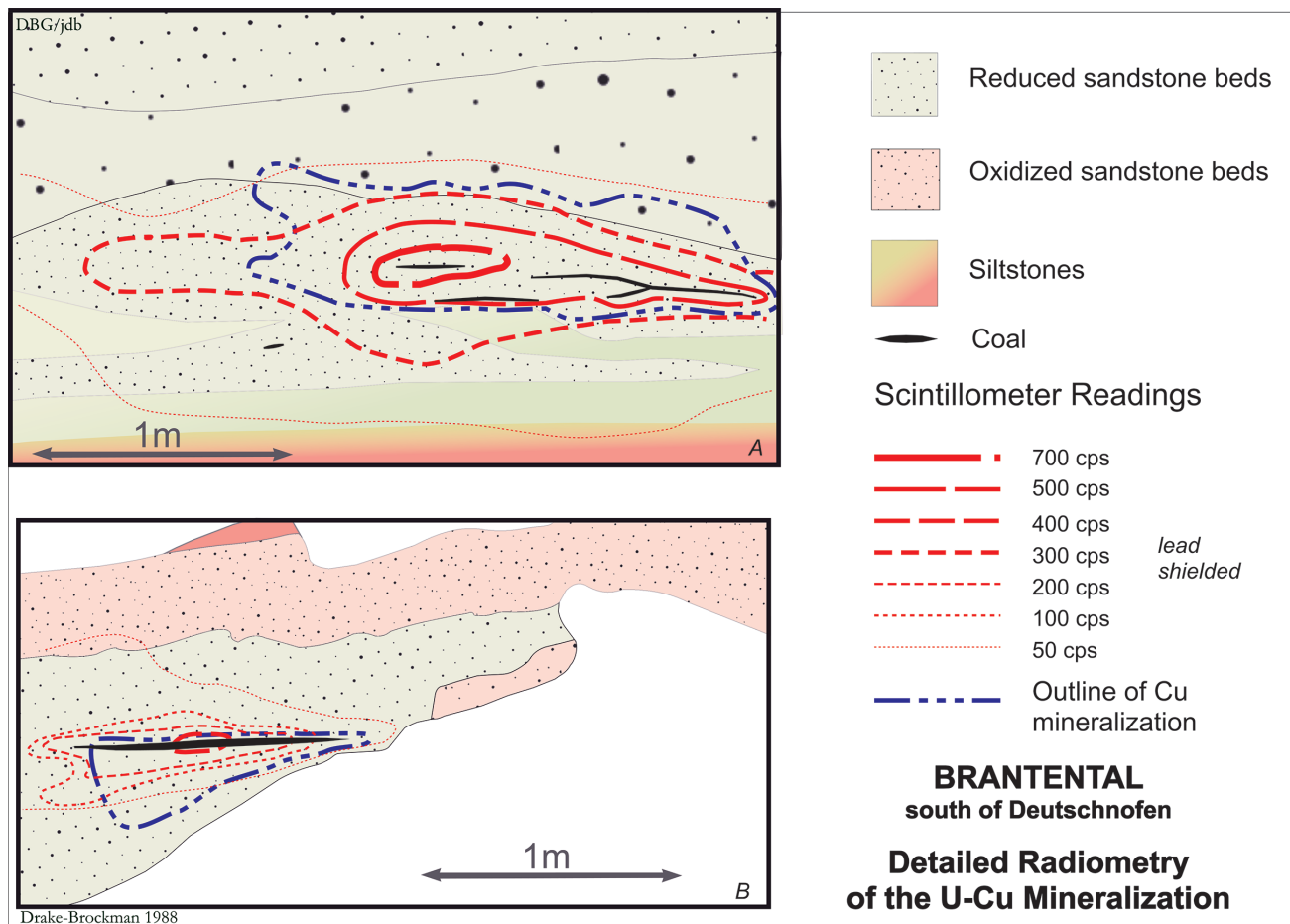
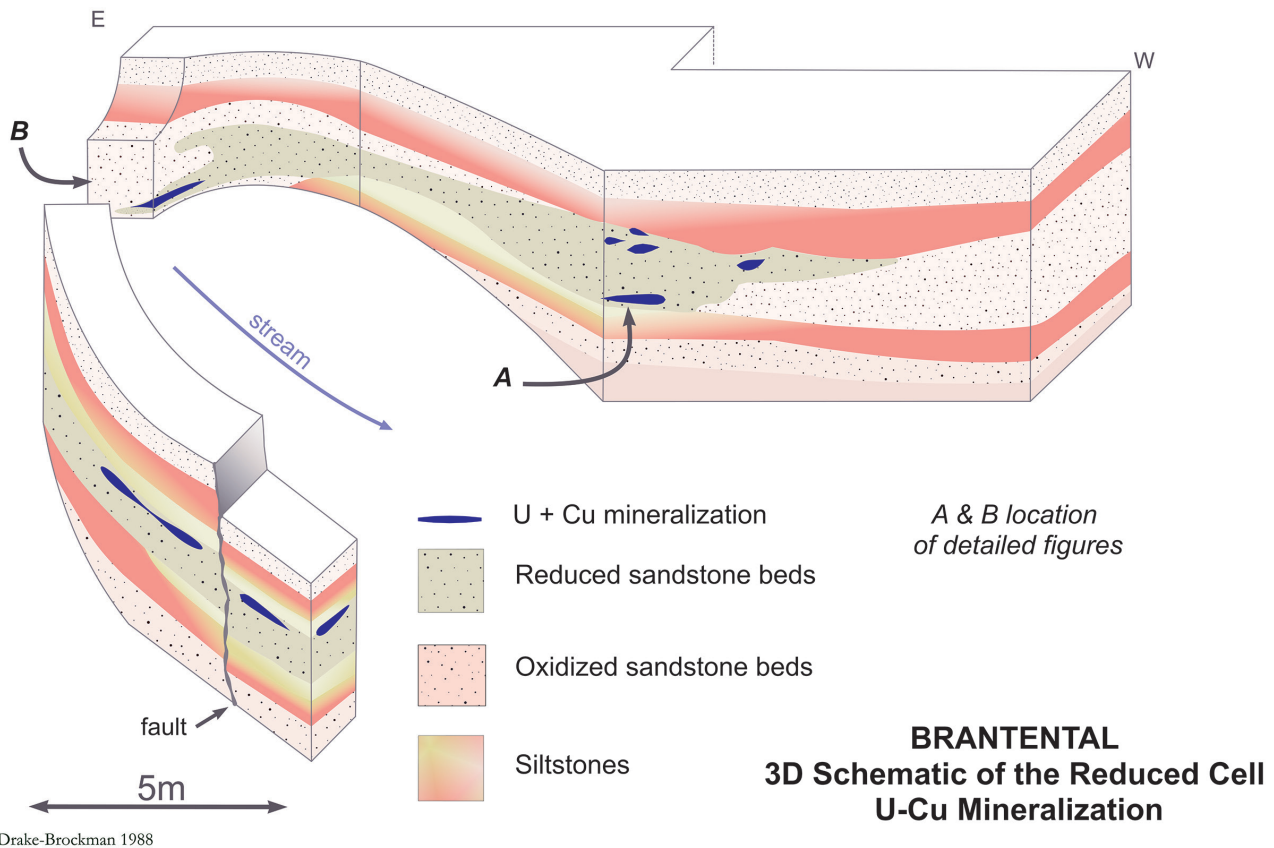
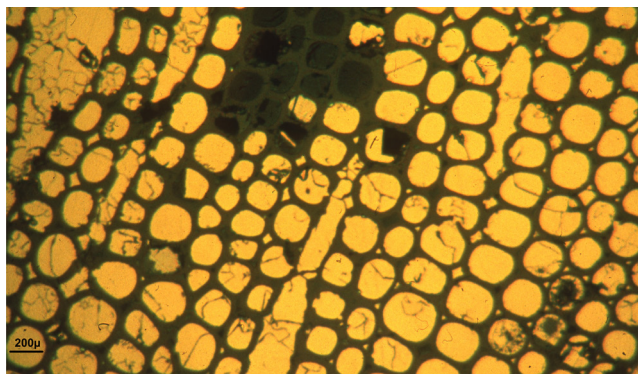


FIG. 9: Examples of Cu and U mineralisation in the upper Brantental. (A) shows how isoradians (lines of equal radioactivity) are extended in the direction of bedding of the mineralized coal seam. (B) demonstrates how the bedding is cut obliquely by the reduction front (modified from Drake-Brockman, 1988).



Drake-Brockman 1988

**FIG. 10:** Block diagram combines the exposures on both sides of the upper Brantental. The position of the reduction front is demonstrated by the colour change from the red of the oxidized sands to the generally greenish or grey hues of those affected by reduction. The most intense mineralisation took place around organic substances which were the foci of reduction. "A" and "B" identifies the positions of the exposures depicted in figures 9A and 9B (modified from Drake-Brockman, 1988).



**FIG. 11:** Microphotograph of coal sample from vicinity of Knappenloch shows completely undeformed lumina of wood cells filled with pyrite. It demonstrates that mineral emplacement occurred prior to compaction and prior to the onset of coalification. (from Griesbecke, 1979).

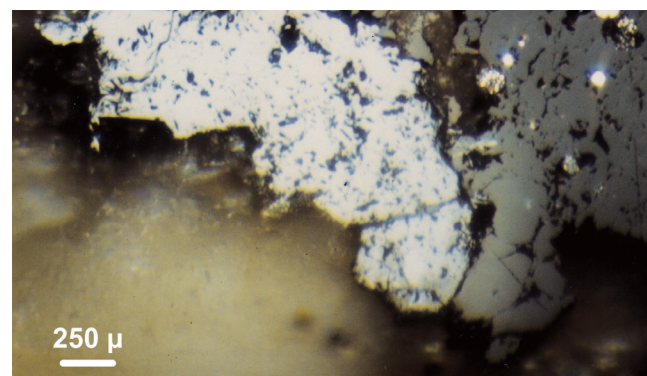
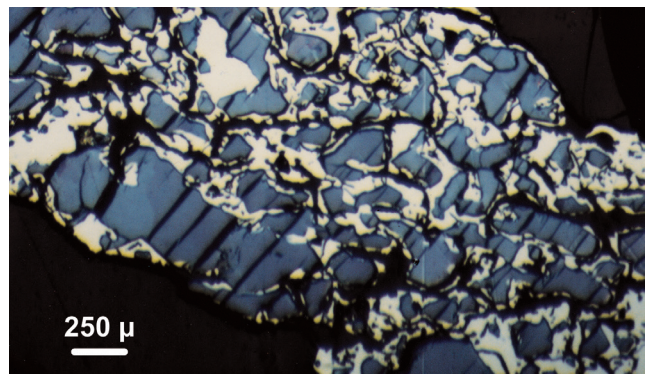


**FIG. 12:** Ore microscopy showing paragenesis of the uranium/copper mineralisation. A: Covellite (blue) is replaced by tennantite (cream). (Brantental, oil, polarized light). B: Uraninite (white) and pyrite (grey) in coal (black) (Moelten, oil, polarized light).

bearing leucoxene) and traces of tennantite (Drake-Brockman, 1988; Drake-Brockman & Wopfner, 1990). Examples of typical ore minerals are shown in figures 12a and 12b. Microprobe analyses of uraninite gave 60–75%  $UO_2$  with no detectable Th or rare earth elements indicating a low temperature origin. The U-Ti mixture gave very variable results of  $UO_2$ : 25–80%,  $TiO_2$  <5–65%,  $PbO$ : 5–10% and  $PO_4$ : <5% which suggests very fine inter-grown material.

Higher up, associated with the first marine ingressions and within sequence 4, lead-zinc mineralisation dominates. The mi-



neralisation occurs within interbedded successions of grey or fawn sandstones and siltstones of distributary channels, often concentrated at the clay draped interfaces of bedding sets. Frequently the mineralisation is bound to masses of washed in plant debris or to carbonaceous siltstones and bituminous sandstones with carbonate nodules which originated in over-bank swamps. On the average, the lead-zinc mineralisation consists of 0.25 mm to 2 mm sized intergrowth of subhedral galena and sphalerite, impregnating the sandstone matrix. Lesser amounts of tennantite occur as blebs along the boundary of galena and sphalerite crystals and often as a matrix between clusters of pyrite crystals and framboids. Microprobe analyses show that sphalerite contains traces of cadmium and occasionally iron. Weathering of galena resulted in skins of both cerrussite and anglesite. An early carbonate cement was precipitated synchronously to the formation of the lead and zinc minerals (Drake-Brockman, 1988).

The stratigraphically lowest lead/zinc concentration occurs just below the cephalopod sandstone, on both sides of the gorge, west of the waterfall at the Butterloch. The mineralised succession measures about 1.5 m and comprises black, carbonaceous siltstone, lenses of coal and bituminous sandstone with typical concretions of slightly dolomitic limestone (Fig. 13). The mineralisation consisting mainly of galena and sphalerite, is disseminated in all lithotypes, but is concentrated around carbonate concretions.

About 25 m stratigraphically above the cephalopod bank, excellent examples of lead mineralisation are exposed where

the Gorz hiking trail crosses the upper part of Bletterbach (Fig. 14). The succession consists of several cycles of fine grained clastics with intercalated, coarse channel sandstones which cut into the supratidal flat. Near the margins of the channels the sandstones contain large lenses of washed in branchlets and other plant debris. The mineral concentrations are bound to these lenses of coalified plant matter, but there is no indication of a redox front and practically no bleaching of the surrounding rocks. Typical associations of ore minerals of this type which are fairly wide spread in the Groeden Sandstone, are depicted in Figures 15a and 15b.

4. DISCUSSION

The low rank of coal indicating thermal exposure of the rocks to values between 60° C and 70° C excludes any participation of hydrothermal fluids on the formation of ore concentrations. Figure 11 shows pyrite, filling completely undeformed cell-lumina of wood enclosed in sedimentary rock of the Bletterbach. Similarly, covellite, tennantite and uraninite also occur as cell filling minerals as described from the Knappenlöcher and other localities (Griesecke, 1979; Drake-Brockman, 1988). Completely undeformed pseudomorphs of pyrite after wood cells in coal from Prissian near Payersbach have also been depicted by Schulz & Fuchs (1991). This provides clear evidence that mineralisation took place during the earliest phase of diagenesis and prior to the compaction of the sediment by loading.

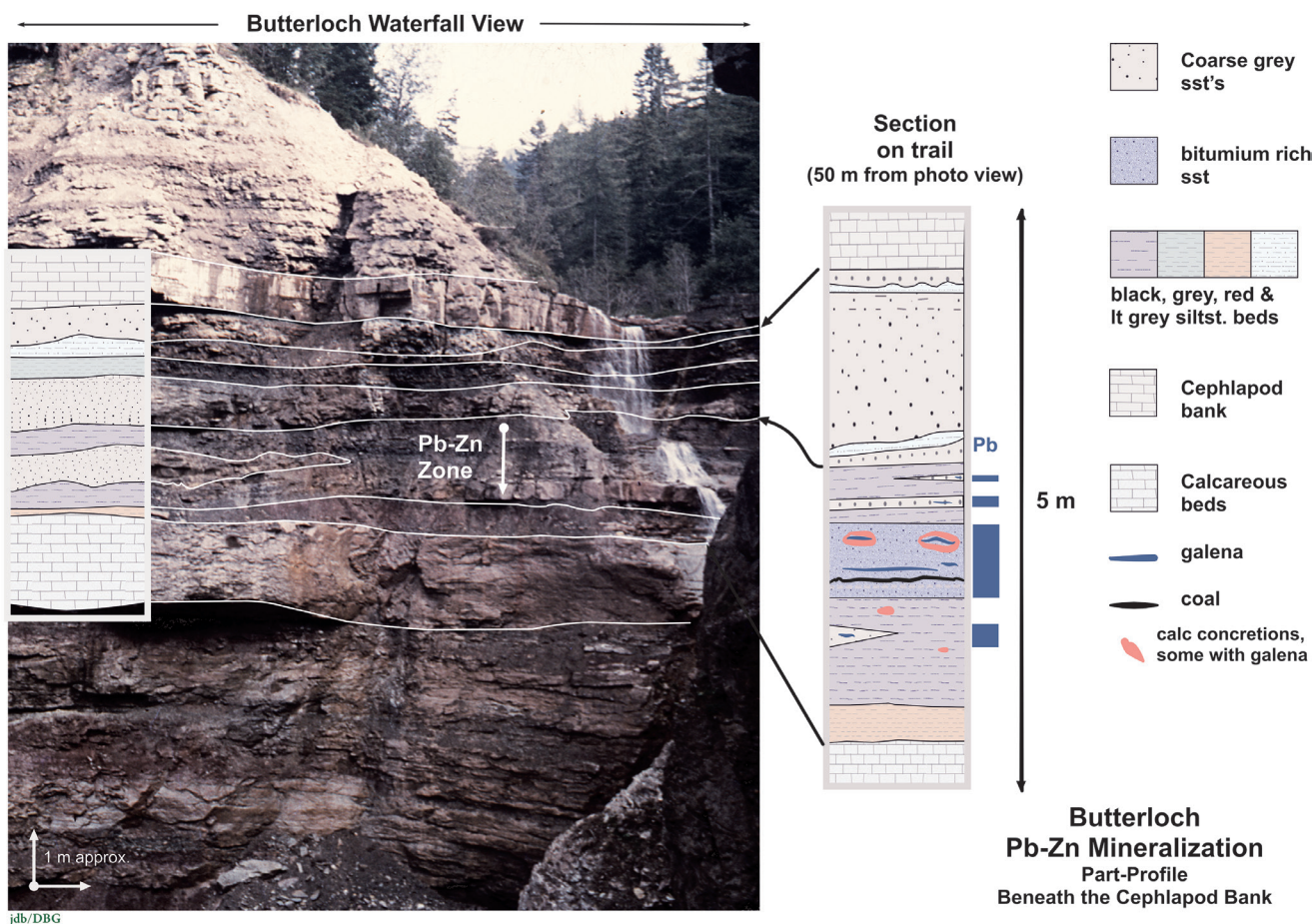


FIG. 13: Carbonaceous siltstones and bituminous mudstones below the cephalopod bed in the surrounding of the Butterloch waterfall in the Bletterbach show intense galena and pyrite mineralisation. The waterfall is visible at the right hand margin of the picture.

It can be stated further that all concentrations of ore minerals are associated with fossil plant material, either as individual tree trunk or as accumulation of plant debris. Thus transportation and concentration of the metals must have been controlled by mechanisms of the sedimentary environment. The low rank of the coal further supports that statement.

During deposition of the lower red bed sequence the groundwaters were dominantly oxidizing and alkaline. However, within channels and overbank swamps, zones of reducing and acid conditions were sustained due to bacterial action in decomposing plant material. At that stage pyrite was precipitated either as 0.01 mm sized framboids or as pyrite "dust" filling the undeformed cell lumina.

As the sediment column increased these reducing cells came under the influence of a regional oxidizing groundwater system. The reduction cells established around the organic remnants contained enough reduction potential to extract, by reduction and absorption uranium and/or copper from the passing groundwater, thereby forming a diffuse reduction front like a halo around the organic matter. These relationships are illustrated in Figures 7, 9 and 10. The mineralisation took place after initial pyrite precipitation, but before compaction and co-alification of the organic material.

Higher up in the succession, especially in sequence 4, lead-zinc mineralisation dominates. It is postulated that the metals were liberated and mobilized during soil formation (see above) and leached out of the rocks of the surrounding source areas by oxidized ground waters.

They were transported in solution down the hydraulic gradients towards trunk drainages and finally into the low lying delta and estuarine plains. Evaporation and extended sediment contact increased concentration from 0.5 ppm to 3 ppm (Baskov, 1983; Mann, 1982a, 1982b). In weak alkaline, saline solutions the solubility threshold for lead and zinc are approached and exceeded by these values. In neutral or acid solutions, the solubility limits are much higher (Mann, 1982a, 1982b). Interaction between the weakly acid to neutral ground waters and the alkaline marine pore waters resulted to a change in pH and in a decrease of solubility of lead and zinc, causing the precipitation of the sulphides. This model is preferred to a simple reduction process because there is no evidence for a controlling redox reaction.

Remains the question to be answered of the original source of the metals. Accumulations of galena, sphalerite and fluorite are not uncommon within the Athesian Volcanic suite. Some of them were mined, even up to recent times (e.g., W of Deutschnofen/Nuova Ponente or Prestavel, NW of Cavalese). However, these provided small amounts of source material compared to the large amounts liberated by weathering and denudation processes during the long hiatus between the volcanics and the Gröden/Val Gardena Sandstone. Mass balance calculations carried out by Griessecke (1979) showed that the weathering of 1 km<sup>3</sup> of acid volcanic rock would liberate 105,300 t of zinc, 51,300 t of lead, 27,000 t of copper and 8,000 t of uranium. The assumed volume of 1 km<sup>3</sup> corresponds to an area of 20 km by 10

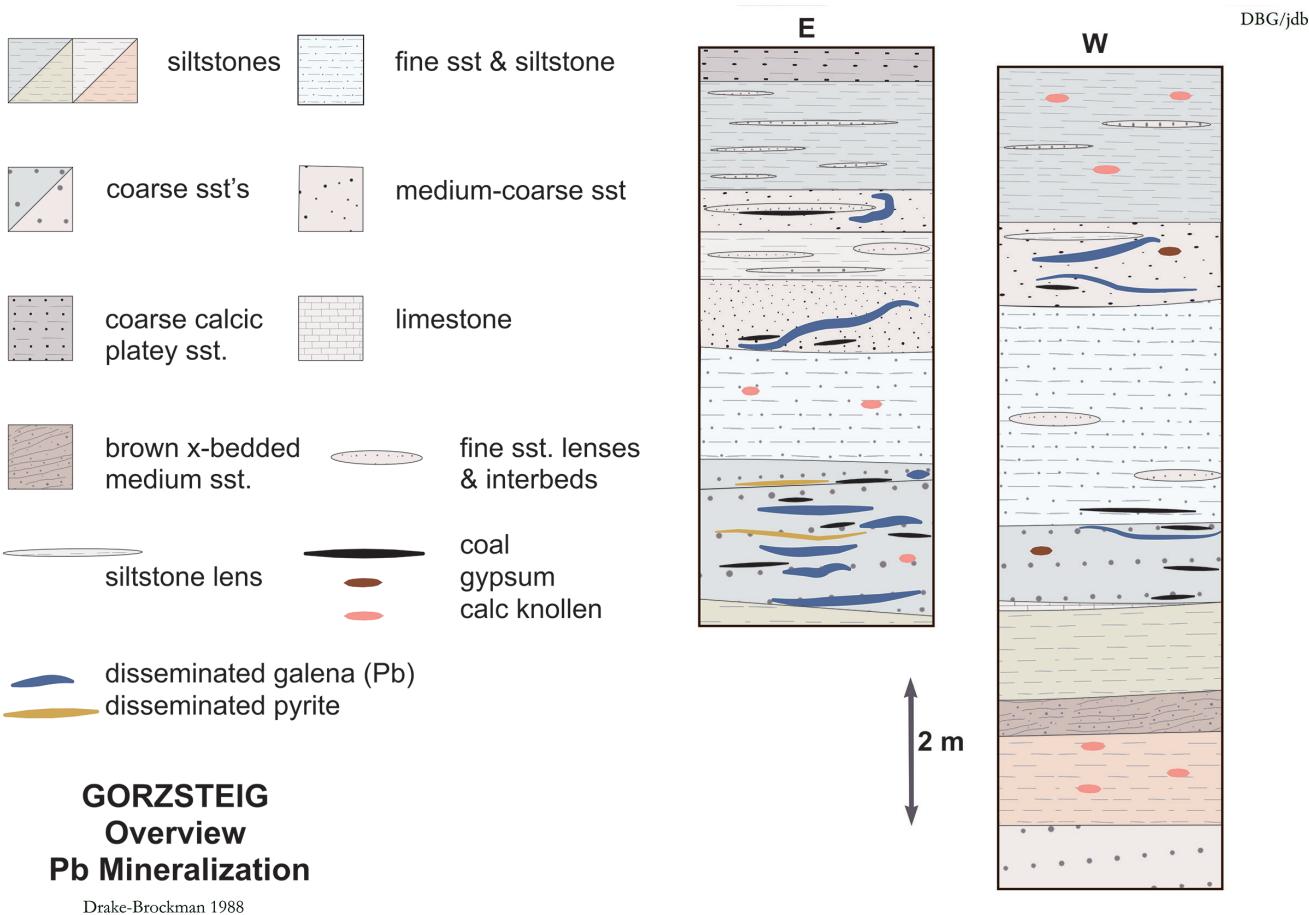


FIG 14: Profiles at the locality Gorzsteig show the interdependence of galena and sphalerite mineralisation and lithology.



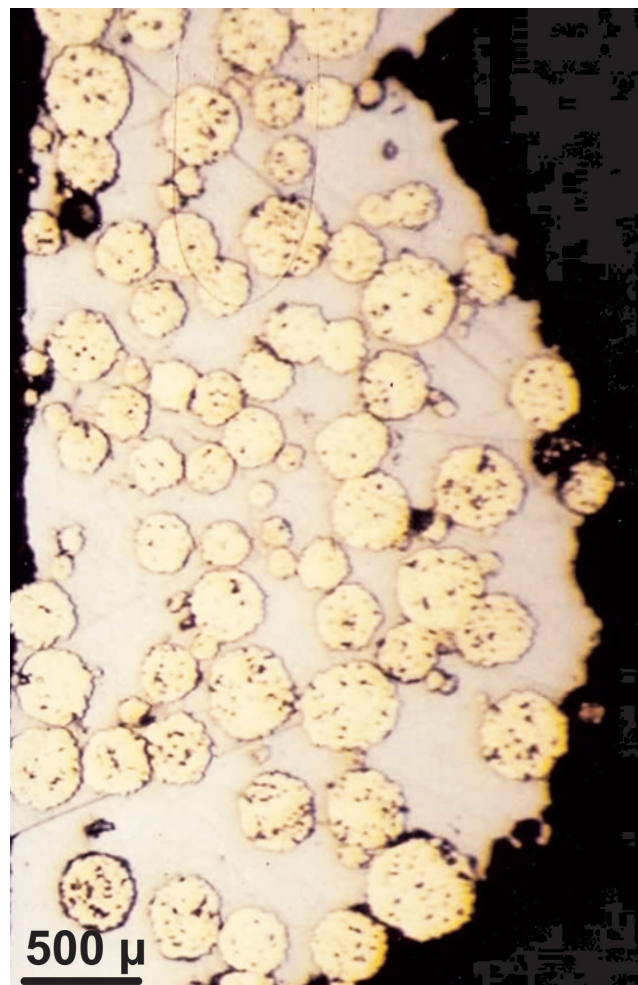
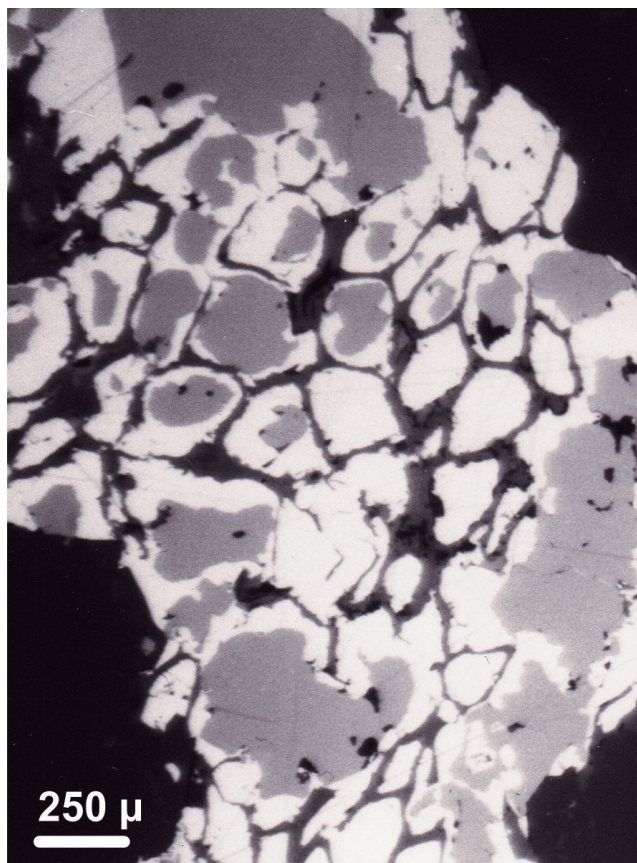


FIG. 15: Ore microscopy of paragenesis of the lead/zinc association. Left: Sphalerite (dark grey) and galena (light grey) fill lumina of wood cells. (Jenesien/San Genesio, oil, polarized light). Right: Pyrite framboids are enclosed by massive galena. (Mölden/Meltina, oil, polarized light).

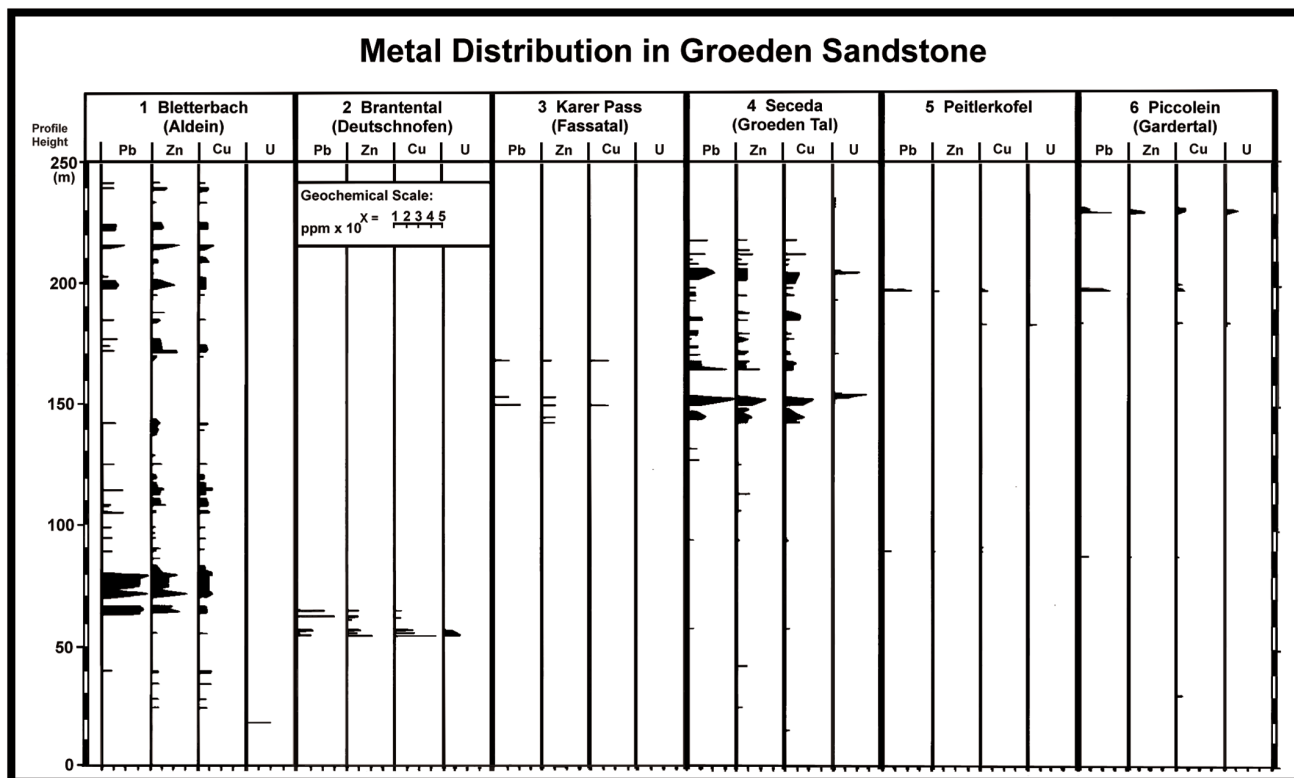


FIG. 16: Geochemistry profiles of Gröden/Val Gardena Sandstone between Bletterbach and Piccolein showing that metal concentrations in the lower parts of the Gröden/Val Gardena Sandstone diminish in a general north-easterly direction. For localities see Figure 1, explanation in text (from Wopfner et al., 1983).

km and a denudation thickness of only 5 m. The actual removal of early Permian volcanic rocks by weathering and denudation during the long intra-Permian hiatus amounted to multiples of the thickness assumed in Griesbeck's model. Thus we may confidently accept that the mayor source for the mineral concentrations in the Gröden/Val Gardena Sandstone were the metals liberated by weathering from the volcanic rocks.

Geochemical investigations of profiles of Gröden/Val Gardena Sandstone beyond the immediate area discussed in this paper are reproduced in figure 16. A comparison between the base metal distribution and the distribution of the reduced facies as identified by Wopfner et al. (1983) reveals a significant correlation. The reduced facies below the transition to the Bellerophon Formation and that associated with the marine ingression of the cephalopod bank show significant lead-zinc mineralisations. Those parts of the Gröden/Val Gardena Sandstone which are dominantly oxidized and do not contain organic matter, or were derived from alluvial fans or braided stream environments as for instance at Peitler Kofel/Sass da Putia, at Rio Barbide or near St. Martin/San Martino are barren or only weakly mineralized. Thus, the increased level of transport energies within the fluvial environments further east apparently deterred mineralization. Torrential type current beds of braided stream systems in the sections around St. Martin/San Martino and the dominance of sheet flood and fan deposits around the Rolle Pass indicate higher gradients and changes of phreatic environments (Wopfner & Farrok, 1988), but also different source areas, like the Cima d'Asta Massif, which already existed as a morphological high at the time of Gröden/Val Gardena Sandstone deposition (Schmitz, 1989). However, widespread Cu and U mineralisation occurred in the Gröden/Val Gardena Sandstone of Slovenia, despite the comparatively high level of depositional energy in braided stream systems which harbour uranium concentrations. Copper ores occur higher up in organic rich mudflat and overbank deposits interleafed in oxidised arenites (Drovenik, 1983; Drovenik et al., 1972; Kober, 1984). This demonstrates the presence of shallow intergranular groundwater flows carrying dissolved metal ions, but according to Drovenik (1983) probably also different source areas in time.

## 5. CONCLUSION

The mineralisation within the Gröden/Val Gardena Sandstone is the product of normal chemical weathering processes in a hot and arid to semi-arid climate. The liberated metal ions were transported by shallow groundwater systems, modified and enhanced en route. Precipitation and enrichment of the metals was achieved by reduction in contact with organic materials and by Eh and pH changes in contact with marine pore waters and again organic matter that influenced the solubility of the dissolved metals. Mineralisation took place during the early stage of diagenesis, prior to compaction and prior to the commencement of coalification.

## REFERENCES

- Andreatta, C. (1959): Aufeinanderfolge der magmatischen Tätigkeiten im größten permisch-vulkanischen Schild der Alpen. – *Geologische Rundschau*, 48: 99–111.
- Baskov, E.A., (1983): The fundamentals of paleohydrogeology of ore deposits. – 253 pp., Springer Verlag, Berlin.
- Bielefeld, D. (1998): Reifebestimmung an Kohlen des Grödner Sandsteins Südtirols, Norditalien. – 85 pp., unpublished diploma thesis, Geologisches Institut der Universität zu Köln.
- Bosselini, A., Hardie, L. (1973): Depositional theme of a marginal marine evaporate. – *Sedimentology*, 20: 5–27.
- Brandner, R., Keim, L. (2011): A 4-day geological field trip in the western Dolomites. – *Geo.Alp*, 8: 76–118.
- Buggisch, W. (1978): Die Grödner Schichten (Perm, Südalpen) Sedimentologische und geochemische Untersuchungen zur Unterscheidung mariner und kontinentaler Sedimente. – *Geologische Rundschau*, 67: 149–180.
- Cassinis, G. (1986): Outline of the Permian geology in the Southern Alps. – In: Società Geologica Italiana (ed.), Field Conference on the Permian and Permian-Triassic Boundary in the South-Alpine segment of the western Tethys, pp. 1–176, Field Guide-Book, Brescia.
- Cassinis, G., Origoni Giobbi, E., Peyronel Pagliani, G. (1975): Osservazioni geologiche e petrografiche sul Permiano della bassa Val Caffaro (Lombardia Orientale). – *Atti dell' Istituto Geologico della Università di Pavia*, 25: 17–71.
- Cassinis, G., Neri, C., Perotti, C.R. (1993): The Permian and Permian-Triassic boundary in eastern Lombardy and western Trentino (Southern Alps, Italy). – In: Lucas, S.G., Morales, M. (eds) *The Nonmarine Triassic*, New Mexico Museum of Natural History and Science Bulletin, 3: 51–63.
- Cassinis, G., Ronchi, A. (2001): Permian chronostratigraphy of the Southern Alps (Italy) - an update. – In: Weiss, R.H. (ed.), *Contributions to Geology and Palaeontology of Gondwana in Honour of Helmut Wopfner*, pp. 73–88, Geologisches Institut der Universität Köln.
- Conti, M.A., Leonardi, G., Mariotti, N., Nicosia, U. (1977): Tetrapod footprints of the "Val Gardena Sandstone" (North Italy). Their palaeontological, stratigraphic and palaeoenvironmental meaning. – *Palaeontographia Italica*, 70: 1–91.
- Dachroth, W. (1988): Gesteinsmagnetischer Vergleich permischer Schichtenfolgen in Mitteleuropa. – *Zeitschrift für geologische Wissenschaften Berlin*, 16: 959–968
- Drake-Brockman, J.A.P. (1988): Mineralisation und Diagenese im Grödner Sandstein, Südtirol, Italien. – 124 pp., Doctoral Thesis, Math. Nat. Fakultät, Universität zu Köln.
- Drake-Brockman, J., Wopfner, H. (1990): Mineralisation and diagenesis in the Groeden Sandstone, South Tyrol, Italy – In: Péllissonnier, H., Sureau, J.F. (eds), *Actes du colloque international " Mobilité et concentration des métaux de base dans les couvertures sédimentaires etc."*, pp. 365–378, Document du BRGM No. 183, Orleans.
- Drovenik, M. (1983): Mineral deposits in Permian and Triassic beds of Slovenia (Yugoslavia). – In: Schneider, H.J. (ed.), *Mineral deposits of the Alps and of the Alpine Epoch in Europe*, pp. 88–96, Springer Verlag, Berlin-Heidelberg.
- Fels, H. (1979): Die sedimentologische Entwicklung der Permabfolge im westlichen Südtirol (N-Italien). – Doctoral Thesis, Sonderveröffentlichungen, Geologisches Institut der Universität zu Köln, 42: 1–145.
- Force, E.R. (1976): Titanium contents and titanium partitioning in rocks. – In: *Geology and resources of titanium*, US Geological Survey Prof. Paper, 959A, B: 1–10.
- Griesbeck, S. (1979): Sedimentologische und geochemische Untersuchungen des Grödner Sandsteins und der basalen Bellerophon-Schichten westlich und nordwestlich des Weißhorns, Südtirol. – 168 pp., unpublished diploma the-



- sis, Geologisches Institut der Universität zu Köln.
- Haditsch, G., Mostler, H. (1974): Mineralisationen im Perm der Ostalpen. – *Carinthia II*, 164(84): 63–71.
- Kober, V. (1983): Sedimentologische und geochemische Untersuchungen des Grödnner Sandsteins in den westlichen Karawanken (NW-Jugoslavien). – 168 pp., unpublished diploma thesis, Geologisches Institut der Universität zu Köln.
- Kober, V. (1984): Zur Genese der Tarviser Breccie in den Karawanken, NW-Jugoslavien. – Doctoral thesis, Geologisches Institut der Universität zu Köln, Sonderveröffentlichungen, 56: 1–155.
- Koch, J. (1979): Die Genese des Grödnner Sandsteines der nordwestlichen Dolomiten (Südtirol, Italien). – Doctoral Thesis, Geologisches Institut der Universität zu Köln, Sonderveröffentlichungen, 43: 1–156.
- Kustatscher, E., van Konijnenburg-van Cittert, J.H.A., Bauer, K., Butzmann, R., Meller, B., Fischer, T.C. (2012): A new flora from the Upper Permian of Bletterbach (Dolomites, N-Italy). – *Review of Palaeobotany and Palynology*, 182: 1–13.
- Mann, A.W. (1982a): Mobility in metal ions. – In: Smith, R.E. (ed.), *Geochemical exploration in deeply weathered terrain*, pp. 97–106, C.S.I.R.O. Work Shop, June, 15–18, Western Australia.
- Mann, A.W. (1982b): Hydrogeochemical facies and regimes of south-western Australia. – In: Smith, R.E. (ed.), *Geochemical exploration in deeply weathered terrain*, pp. 118–127, C.S.I.R.O. Work Shop, June, 15–18, Western Australia.
- Massari, F., Neri, C., Pittau, P., Fontana, D., Stefani, C. (1994): Sedimentology, Palynostratigraphy and sequence stratigraphy of a continental to shallow-marine rift-related succession: Upper Permian of the eastern Southern Alps (Italy). – *Memorie di Scienze Geologiche Padova*, 46: 119–243.
- Mauritsch, H.J., Becke, M. (1983): A magnetostratigraphic profile in the Permian (Gröden Beds, Val Gardena Formation) of the Southern Alps near Paularo (Carnic Alps, Friuli, Italy). – *Newsletter IGCP*, 5: 80–86.
- Menning, M. (2001a): The Permian Illawarra Reversal in SE-Australia as global correlation marker versus K-Ar ages and palynological correlation. – In: Weiss, R.H. (ed.), *Contributions to geology and palaeontology of Gondwana in Honour of Helmut Wopfner*, pp. 325–332, Geologisches Institut der Universität zu Köln,
- Menning, M. (2001b): A Permian Time Scale 2000 and correlation of marine and continental sequences using the IL-LAWARRA Reversal (265 Ma). – In: Cassinis, G. (ed.), *Monographia di Nature Bresciana, Museo Civico di Scienze Naturali di Brescia*, 25: 355–362.
- Mitterpergher, M. (1974): Genetic characteristics of uranium deposits associated with Permian sandstones in the Italian Alps, formation of uranium ore deposits. – 299 pp., International Atomic Energy Agency, Vienna.
- Mutschlechner, G. (1933): Cephalopodenfauna im Grödnner Sandstein. – *Verhandlungen der Geologischen Bundesanstalt Wien*, 11: 1–136.
- Nicosia, U., Sacchi, E., Spezzamonte, M. (2001): New palaeontological data from the Val Gardena Sandstone. – In: Cassinis, G. (ed.), *Permian continental deposits of Europe and other areas. Regional Reports and correlations, Monographia di Nature Bresciana, Museo Civico di Scienze Naturali di Brescia*, 25: 83–88.
- Press, S. (1982): Zur Geochemie mariner und terrestrischer Sedimente und deren Färbung. – Doctoral Thesis, Geologisches Institut der Universität zu Köln, Sonderveröffentlichungen, 44: 1–209.
- Schmitz, M. (1989): Sedimentologischer Nachweis eines südlichen Liefergebietes für den Grödnner Sandstein am Passo Rolle. – *Geologische und Paläontologische Mitteilungen Innsbruck*, 16: 101–104.
- Schulz, O., Fuchs, H.W. (1991): Kohle in Tirol: Eine historische, kohlenpetrographische und lagerstättenkundliche Betrachtung. – *Archiv für Lagerstättenforschung*, 13: 123–213.
- Societa Geologica Italiana (1986): *Field Guide – Book*. – 176 pp., Field conference on Permian and Permian-Triassic Boundary in the South-Alpine Segment of the western Tethys. Brescia, Italy.
- Uhl, D., Butzmann, R., Fischer, T.C., Meller, B., Kustatscher, E. (2012): Wildfires in the Palaeozoic and Mesozoic of the Southern Alps – the late Permian of the Bletterbach-Butterloch area (northern Italy). – *Rivista Italiana di Palaeontologia and Stratigraphia*, 118: 223–233.
- Venturini, C. (1990): *Geologia delle Alpe Carniche centro orientali*. – *Museo Friulano di Storia Naturale, Udine*, 38: 1–220.
- Wartmann, R., Knatz, H. (1977): Petrographische Untersuchungen an Kohlen- und Sandsteinproben aus dem «mittel»-permischen Grödnner Sandstein der westlichen Dolomiten. – 8 pp., Bergbauforschung GmbH., unpublished report, Essen.
- Wopfner, H. (1984): Permian deposits of the Southern Alps as product of initial Alpidic taphrogenesis. – *Geologische Rundschau*, 73: 259–277.
- Wopfner, H., Farrokh, F. (1988): Palaeosols and heavy mineral distribution in the Gröden Sandstone of the Dolomites. – *Memorie della Società Geologica Italiana*, 34: 161–173.
- Wopfner, H., Griessecke, S., Koch, J., Fels, H. (1983): New aspects on metal deposits of the Gröden Sandstone (South Tyrol, Italy). – In: Schneider, H.J. (ed.), *Mineral deposits of the Alps and of the Alpine Epoch in Europe*, pp. 60–69, Springer, Berlin-Heidelberg.
- Wopfner, H., Höcker, C.F.W. (1987): The Permian Gröden Sandstone between Bozen and Meran (northern Italy). A habitat of Dawsonite and Nordstrandite. – *Neues Jahrbuch für Geologie und Paläontologie, Monatshefte*, 3: 161–176.

#### ARTICLE HISTORY

Received 28 June 2017

Received in revised form 11 September 2017

Accepted 10 October 2017

Available online 31 December 2017